Journal of Photonics for Energy

PhotonicsforEnergy.SPIEDigitalLibrary.org

Numerical modeling of a four-rod pumping scheme for improving TEM_{00}-mode solar laser performance

Joana Almeida
Dawei Liang
Bruno D. Tibúrcio
Dário Garcia
Cláudia R. Vistas

SPIE.

Joana Almeida, Dawei Liang, Bruno D. Tibúrcio, Dário Garcia, Cláudia R. Vistas, "Numerical modeling of a four-rod pumping scheme for improving TEM_{00}-mode solar laser performance," *J. Photon. Energy* **9**(1), 018001 (2019), doi: 10.1117/1.JPE.9.018001.

Numerical modeling of a four-rod pumping scheme for improving TEM_{00}-mode solar laser performance

Joana Almeida, Dawei Liang,* Bruno D. Tibúrcio, Dário Garcia, and Cláudia R. Vistas

Universidade NOVA de Lisboa, Faculdade de Ciências e Tecnologia, Centro de Física e Investigação Tecnológica, Departamento de Física, Campus de Caparica, Portugal

Abstract. A four-rod solar pumping concept is proposed for the significant improvement in TEM_{00}-mode solar laser performance. A quadrangular pyramidal reflector is used to separate the focused solar rays from a 2.0-m diameter parabolic mirror into four focal spots. Four laser heads, each one consisting of a double-stage biconical lens/conical pump cavity and a small diameter Nd:YAG rod, are placed at each of the four focal zones. TEM_{00}-mode laser output of 7.22 W is numerically obtained from each rod, resulting in 28.9 W (4×7.22 W) total TEM_{00}-mode power from the four-rod scheme with 9.41 W/m^2 collection efficiency. This value is 2.5 times more than that of the numerically calculated laser power collection efficiency from a single-rod pumped by the same parabolic mirror. A brightness conversion efficiency of 0.86% is achieved. Substantial improvements in TEM_{00}-mode solar laser stability and thermal performance are also numerically demonstrated. © *2019 Society of Photo-Optical Instrumentation Engineers (SPIE)* [DOI: 10.1117/1.JPE.9.018001]

Keywords: solar laser; four-rod; solar pumping; TEM_{00}-mode; parabolic mirror; Nd:YAG.

Paper 18135 received Nov. 26, 2018; accepted for publication Jan. 29, 2019; published online Feb. 20, 2019.

1 Introduction

Solar-powered lasers are considered a promising technology. By directly converting incoherent and broadband solar radiation into coherent and narrowband laser radiation, solar lasers may offer simplicity and reliability for space-based applications, leading to a significant decrease in the cost of laser production. Among the potential space applications are deep space and space-to-Earth power transmission,[1] fuel-free photonic thrusters, asteroid deflection,[2] and removal of orbital space debris.[3] Solar lasers have also large potential for terrestrial applications, offering a renewable alternative energy solution in sun-rich countries. Particular attention has been paid to the renewable magnesium (Mg)–hydrogen (H_2) cycle,[4] which may lead to a fuel-free, energy-efficient, and cost-effective Mg-based transport system.

Solar lasers have a +50 year history. The first report occurred in 1963 by Kiss et al.,[5] not long after the invention of the laser.[6] Shortly thereafter, Young succeeded in demonstrating the first 1 W continuous-wave (CW) Nd:YAG solar laser emission.[7] After Young's work, there was little progress until 1984, when the solar laser power was increased to 18 W by Arashi et al.[8] In the meantime, liquid and gas laser media have also been explored as candidates for solar lasers.[9–11] However, solar laser research has essentially converged to systems with solid-state media[12–29] due to their inherent high energy density, compactness, and potential for efficient solar-to-laser power conversion.

In the first Nd:YAG solar systems, efforts were made to increase the laser output power,[7,8,12] from 1.0 W in 1966[7] to 60.0 W in 1988,[12] all pumped by a primary parabolic mirror. One of the most important parameters for the assessment of solar laser is its collection efficiency—defined as the solar laser output power per unit collection area—which was not seriously considered until 1996 by Jenkins et al.,[13] who reported a collection efficiency of 4.5 W/m^2. Since then, solar laser researchers have continued to improve the collection efficiency using either parabolic

*Address all correspondence to Dawei Liang, E-mail: dl@fct.unl.pt

mirror[14–19] or Fresnel lens[20–25] primary collectors. The current record in solar laser collection efficiency is 32.5 W/m^2 by end-side-pumping a 4.5-mm diameter, 35-mm length Cr:Nd:YAG laser rod through NOVA heliostat–parabolic mirror system, with a liquid light guide lens as a secondary concentrator.[19] The improvement of solar laser efficiency by adding Cr^{3+} ions as a codopant in Nd:YAG was carried out in 2007,[20] since it provides a broader absorption band than Nd:YAG for capturing sunlight.[30,31] Still, the preceding attempts to increase the solar laser efficiency with chromium codoping resulted in a little more than 10% increase in efficiency.[23]

In addition to laser efficiency, laser beam quality is also of practical importance to evaluate laser output performance. It was not until 2003 that the solar laser beam quality measurements were conducted by Lando et al.,[14] who defined the brightness figure of merit—the ratio between laser power and the product of M_x^2 and M_y^2 beam quality factors. Even so, substantial improvement in brightness figure of merit was only achieved in 2013, through the first TEM_{00}-mode laser operation, by side-pumping a 3.0-mm diameter Nd:YAG rod with a Fresnel lens installed on a solar tracker.[26] The choice of a large-mode volume resonator configuration was essential for the maximum extraction of 2.3 W cw TEM_{00}-mode ($M^2 \leq 1.1$) power, reaching 1.9-W brightness figure of merit. Gaussian TEM_{00}-mode beam produces the smallest beam divergence, the highest power density, and thus the highest brightness and the ability to be focused to a diffraction-limited spot.[32] For these reasons, it is the most commonly used laser beam shape in material processing,[33] being also highly desirable for the above-mentioned solar laser applications. The laser beam quality, and thus the beam brightness, also depends heavily on rod diameter. Since the rod acts as an aperture, by pumping a small diameter laser rod, high-order resonator modes can be suppressed by large diffraction losses, and beam quality improves. Laser rods of small diameter are also more resistant to thermal stress. For these reasons, since the first TEM_{00}-mode solar laser operation,[26] our research group has been insisting on improving the TEM_{00}-mode laser efficiency and brightness by pumping a small diameter laser rod within a large-mode volume resonator.[18,27–29,34] For this purpose, parabolic mirrors have been used as primary concentrators since they can concentrate the sunlight into a small focal spot without chromatic or spherical aberration, thus pumping more efficiently a small diameter laser rod. TEM_{00}-mode solar laser performance is commonly characterized by TEM_{00}-mode collection efficiency and beam brightness figure of merit. Nevertheless, these two definitions may be misleading since both depend on solar irradiance, which can vary largely with geographical location. Therefore, for the correct evaluation of the TEM_{00}-mode laser performance, we introduce here a definition—the brightness conversion efficiency, i.e., laser beam brightness figure of merit divided by incoming solar power. The advances in TEM_{00}-mode collection efficiency, brightness figure of merit, and brightness conversion efficiency are shown in Fig. 1.

Fused silica light-guides were proposed and tested to pump uniformly either a 3.0-mm diameter[27] or a 4.0-mm diameter,[28] 30-mm length, Nd:YAG rod, resulting in 4.0 W beam brightness[27] and 5.5 W TEM_{00}-mode power.[28] The collection efficiencies were lower than that of the first TEM_{00}-mode solar laser,[26] which are due to the low light coupling efficiency between the output end of the light guide and the laser rod.[27,28] Therefore, direct side-pumping configurations were subsequently tested, where the concentrated solar radiation at the focus was more efficiently coupled within the laser rod, through either a fused silica cylindrical lens[29] or a fused silica ellipsoidal-shaped lens.[34] As observed in Fig. 1, most of the TEM_{00}-mode solar laser prototypes had side-pumping configuration.[26–29] This configuration is effective for power scaling as it allows a more uniform absorbed pump profile along the laser medium, becoming less sensitive to high pump power fluctuations. Substantial progress in TEM00-mode power, collection efficiency, and beam brightness figure of merit was, however, registered in 2017 by end-side-pumping a 4.0-mm diameter, 35-mm length, 1.0 at. % Nd:YAG rod.[18] The TEM_{00}-mode collection efficiency was almost doubled, reaching 7.9 W/m^2. Record-high beam brightness of 6.46 W was achieved, being 1.62 times more than the previous value.[34]

Enhancements in TEM_{00}-mode collection efficiency were achieved with PROMES-CNRS (Procédés, Matériaux et Énergie Solaire—Centre National de la Recherche Scientifique) parabolic mirror in 2016[34] and 2017.[18] It is worth noting that these last results were obtained using only the central part of the parabolic mirror, to achieve high laser efficiency and also avoid overheating the Nd:YAG medium. The increase of the collection area not only degraded the collection efficiency but also precluded the emission of TEM_{00}-mode laser.

Year	2013 [26]	2015 [27]	2016 [34]	2017 [18]
Primary concentrator	Fresnel lens	Parabolic mirror	Parabolic mirror	Parabolic mirror
Effective collection area	0.64 m^2	2.30 m^2	1.13 m^2	1.18 m^2
Incoming solar power	724 W	1890 W	1042 W	1186 W
Pumping configuration	Side pumping	Side pumping	Side pumping	End-side pumping
Laser head	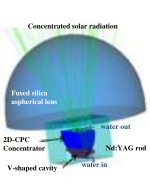	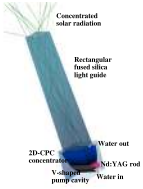	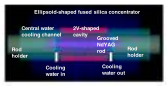	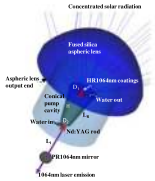
TEM_{00}-mode power	2.3 W	4.4 W	4.5 W	9.3 W
TEM_{00}-mode collection efficiency	2.9 W/m^2	1.9 W/m^2	4.0 W/m^2	7.9 W/m^2
Brightness figure of merit	1.9 W	4.0 W	3.72 W	6.46 W
Brightness conversion efficiency	0.26%	0.20%	0.36%	0.55%

Fig. 1 TEM_{00}-mode solar laser performances.

An alternative four-rod solar pumping approach is presented here to improve the TEM_{00}-mode laser performance, significantly, while taking advantage of using the full primary concentrator area. The concentrated solar rays from the parabolic mirror were separated by a quadrangular pyramidal reflector, forming four identical focal spots. Four solar laser heads, each composed of a biconical lens and a hollow conical pump cavity, within which a small diameter laser rod was positioned, were then placed individually at each focal zone. Efficient pumping of small diameter laser rods with reduced thermal lensing effects was hence ensured. Large improvement in TEM_{00}-mode solar laser performance was numerically achieved. About 28.9 W (4×7.22 W) total TEM_{00}-mode power was numerically obtained from the four-rod scheme, resulting in collection efficiency of 9.41 W/m^2. This was 1.19 times more than the previous experimental record.[18] About 0.86% brightness conversion efficiency was also numerically calculated, representing a 1.56 times improvement over the previous experimental record.[18] This value was also 2.26 times more than that of the numerically calculated brightness conversion efficiency from a single-rod pumped by the same parabolic mirror. Improved TEM_{00}-mode solar laser beam stability and its reduced dependency on the variation of solar irradiance were numerically verified. Improvement in TEM_{00}-mode thermal performance was also numerically demonstrated.

2 Four-Rod Solar Laser Pumping Approach

2.1 *Solar Energy Collection and Concentration System*

The PROMES-CNRS solar energy collection and concentration system was composed of a large plane mirror (with 36 flat segments), mounted on a two-axis heliostat, which redirected the incoming solar radiation toward a stationary parabolic mirror with 2-m diameter, 60-deg rim angle, and 850-mm focal length.[15,16,18] By discounting the central hole area of the parabolic mirror (represented in Fig. 2), an effective collection area of 3.07 m^2 was considered. All the mirrors were back-surface silver coated. Due to iron impurities within the glass substrates of plane and parabolic mirrors, along with >70 years usage, considerable absorption losses occur when the incoming radiation was redirected and focused by these mirrors. So, only 59% reflectivity was effectively measured at the focal zone[16] and, thus, considered in the numerical simulations. Considering the typical solar irradiance of 1000 W/m^2 in Odeillo (France), more than 1800 W solar power can be focused into a highly concentrated pump light spot with near-Gaussian distribution of 11 mm full width at half maximum (FWHM).[15,16]

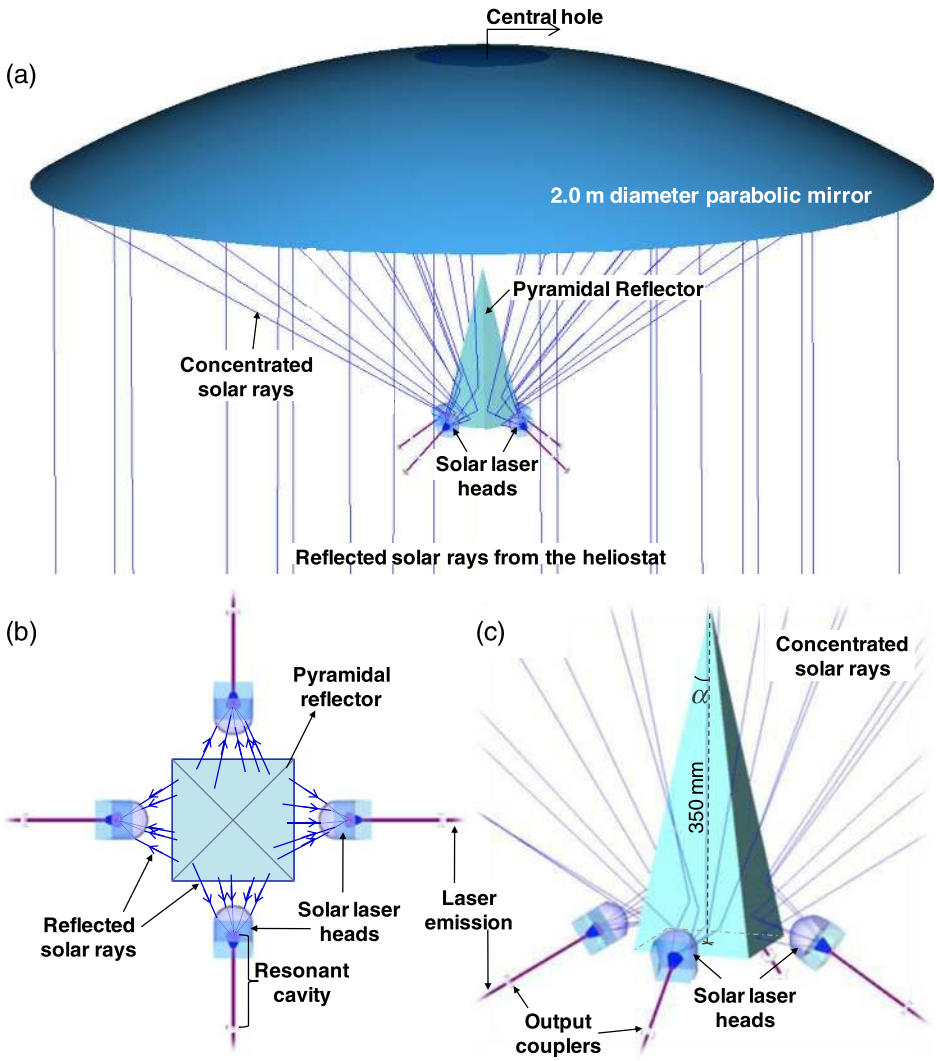

Fig. 2 (a) Four-rod solar pumping approach. (b) Top-view and (c) 3-D detailed view of the four laser heads around the pyramidal reflector. Here, α represents the semivertex angle.

2.2 *Four-Rod TEM_{00}-Mode Solar Laser Pumping Scheme*

The proposed four-rod pumping system for high efficiency TEM_{00}-mode solar laser is shown in Fig. 2. The collected solar rays from the heliostat were first focused by the 2.0-m diameter parabolic mirror [Fig. 2(a)]. A quadrangular pyramidal reflector with 350-mm height and 10-deg semivertex angle α [Fig. 2(c)] was used to evenly separate the highly concentrated rays into four focal spots with 8.4-mm FWHM. A 98% front-surface coating on the pyramid surfaces was considered, ensuring about 440 W solar power onto each focal spot.

The four Nd:YAG laser heads were then placed at their respective focal zone for the efficient end-side-pumping of a small diameter Nd:YAG rod. Each laser rod was pumped by only one-quarter of the total primary collection area; a lower solar pumping power was injected on the laser rod when compared to the classical solar laser schemes.[7,8,12–29]

2.3 *End-Side Pumping Approach for the Single-Laser Head*

As shown in Fig. 3, each solar laser head was composed of two simple stages: the biconical fused silica lens and the hollow conical-shaped pump cavity, within which the 3.0-mm diameter (D_{ROD}), 20-mm length (L_{ROD}), 1.0 at. % Nd:YAG rod was positioned.

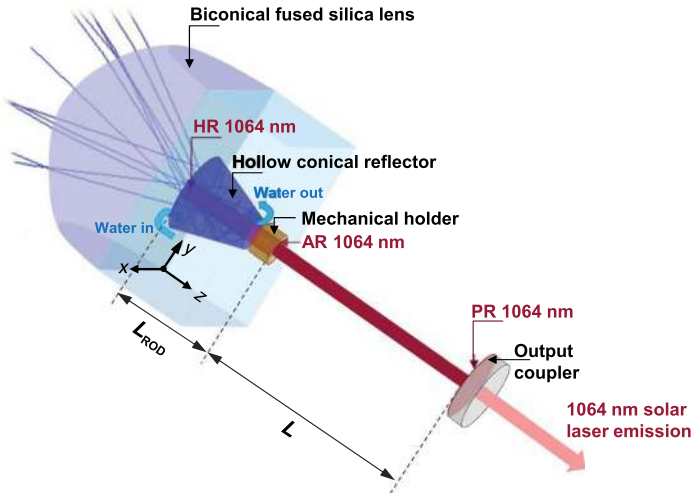

Fig. 3 Single-laser head of the four-rod scheme, composed of the biconical lens, the Nd:YAG rod, and the conical pump cavity. The high reflection (HR 1064 nm) coating on the upper end face of the laser rod and the partial reflection (PR 1064 nm) on the output mirror, together with the laser rod, formed the laser resonator. Here, L represents the separation length between the antireflection (AR 1064 nm) coating on the end face of the rod and the PR 1064 nm on the output mirror.

The biconical fused silica lens collected and compressed the concentrated solar radiation from the pyramidal reflector into the laser rod. The biconical lens was 28 mm in height and 40 mm in width in both X and Y axes, and the radius of curvatures R_x and R_y were 17.7 mm and 20.0 mm, respectively, to guarantee a nearly symmetric pump profile. For end-pumping, one part of the concentrated radiation was directly focused onto the high reflection (HR 1064 nm) coating at the upper end face of the rod by the biconical lens (Fig. 3). The HR 1064-nm coating reflected the laser radiation within the resonator cavity but permitted the passage of other solar pumping wavelengths. For side-pumping, another part of the radiation was guided into the hollow conical cavity with 16/6.5 mm input/output diameters, respectively, and 14-mm height. The zigzag passage of the rays within the hollow pump cavity ensured the multipass side-pumping into the rod,[15–19] as observed in Fig. 3. The inner wall of the pumping cavity was bonded with a protected silver-coated aluminum foil with 95% reflectivity. The Nd:YAG rod was actively cooled by water. The water flow directions are indicated by the arrows in Fig. 3. The water first passes through the space between the output face of the biconical lens and the input face of the conical pump cavity, first cooling the top end of the laser rod. It then passes inside the hollow conical pump cavity, cooling the sidewall faces of the rod, until it finally exits the laser head through the space between the output section of the pump cavity and the mechanical holder. Due to the small overlap of only 16% between the absorption spectrum of the Nd:YAG material and the solar emission spectrum,[35] the maximum contact between the coolant and the rod is essential for the removal of the generated heat. Water is an excellent coolant for solar lasers since it has a high thermal conductivity, specific heat, and low viscosity. In addition to, since the refractive index of water ($n_{\text{water}} \approx 1.33$) is lower than that of fused silica ($n_{\text{silica}} \approx 1.46$), the direct contact of the biconical lens output face with water ensured the efficient light coupling into the rod.

3 Numerical Optimization of the Four-Rod Scheme

3.1 *Optimization of the Optical Design Parameters Through ZEMAX® Ray Tracing*

Similar to our previous solar schemes,[15–19] all the above-mentioned design parameters of the four-rod approach were first optimized by nonsequential ray-tracing ZEMAX® software, achieving a compromise between absorbed pump power and absorbed pump profile within the laser rod. The standard solar spectrum for one-and-a-half air mass (AM1.5)[36] was used

as the reference data for consulting the spectral irradiance ($W/m^2/nm$) at each wavelength of the solar spectrum.

A typical terrestrial solar irradiance of 1000 W/m^2 in Odeillo area (France) on clear sunny days was considered in ZEMAX®.[18] The effective pump power of the light source took into account the overlap between the absorption spectrum of the active medium and the solar emission spectrum, which is 16% for the Nd:YAG material.[35] Spectral variation such as reflectance and transmission through the heliostat, parabolic mirror, and pyramidal reflector were programmed. The absorption spectrum and the wavelength-dependent refractive indexes of fused silica and water were also included in the glass catalog data of ZEMAX®. The influence of the semi-vertex angle of the pyramidal reflector on both the focal distance and pump intensity was numerically studied, as shown in Fig. 4. As the pyramidal semi-vertex angle decreased, the focal distance became shorter [Fig. 4(a)], and the peak flux increased [Fig. 4(b)], but it was more difficult to place the laser head near the pyramidal reflector. This impaired the biconical lens efficiency in compressing the concentrated solar rays to the laser rod. In Fig. 4(b), it is possible to observe a nearly symmetric profile at the focal zone (Z_f). However, a nonsymmetric pump distribution is noticed as the distance Z decreases or increases from $Z_f = 90$ mm, becoming larger at the X-axis, as illustrated in Fig. 5.

The adoption of the biconical lens, instead of the typical aspherical lens[16–18] in end-side-pumping configurations, was essential to compensate the nonsymmetry of the concentrated solar radiation in Figs. 5 and 6(a). Figure 6 shows the pump-flux distributions along five transversal cross sections and one longitudinal central cross section of the laser medium pumped through either an aspherical lens [Fig. 6(a)] or the biconical lens [Fig. 6(b)].

Red color means near maximum pump absorption, whereas blue means little or no absorption. A more symmetrical absorbed pump profile was obtained by the laser rod pumped through the biconical lens, as observed by the transversal cross-section at the top of the laser rod [Fig. 6(b)]. Moreover, the use of the biconical lens also offered a more uniform absorbed pump profile along the laser rod when compared with that of aspherical lens. The absorbed pump peak intensity was reduced by about 15%, reducing the thermally induced effects. From solid-state laser medium, Nd:YAG is by far the most commonly used in solar-pumped lasers.[7,8,12–29,34] It possesses a combination of properties favorable for laser operation. Despite the small overlap

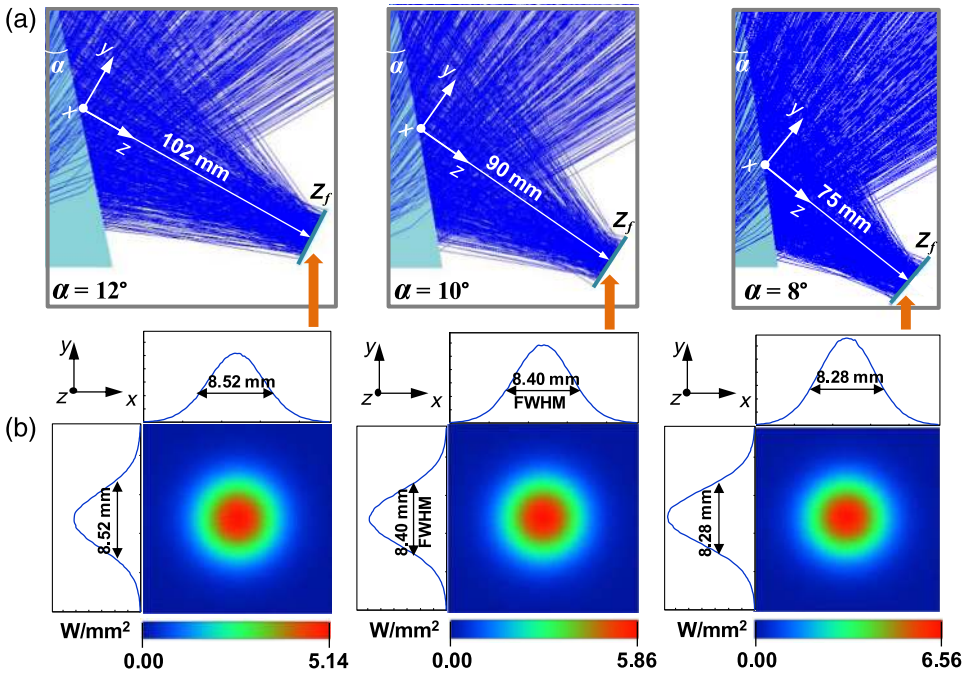

Fig. 4 (a) Detailed view of the concentrated solar light redirected on one side of the pyramidal reflector, at three different semivertex angles and (b) their respective profiles. Here, Z_f indicates the Z-position of the focal zone.

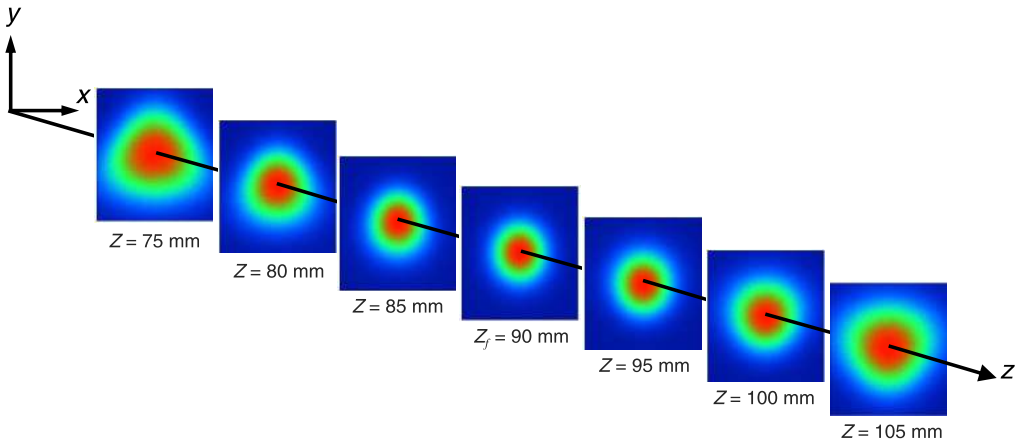

Fig. 5 Pump light distribution along the Z-axis.

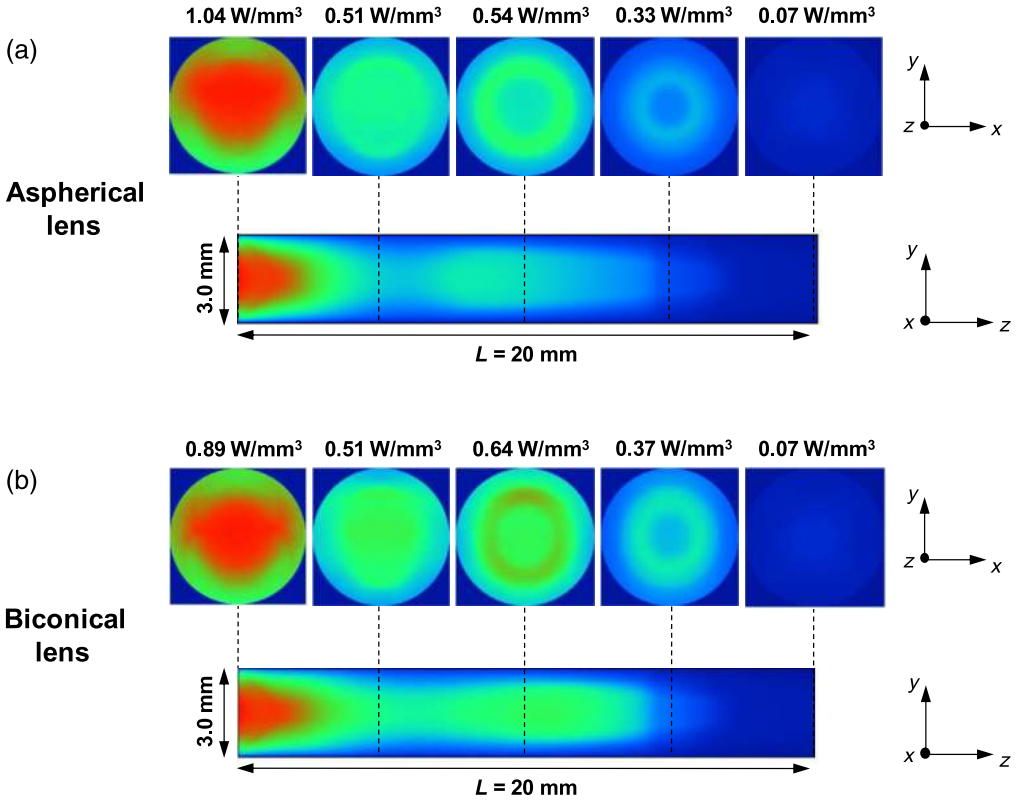

Fig. 6 Numerical absorbed pump flux distributions along the central and longitudinal cross sections of the 3.0-mm diameter, 20-mm length, 1.0 at. % Nd:YAG rod pumped through the four-rod scheme, with (a) aspheric lens and (b) biconical lens.

between the Nd:YAG absorption spectrum and the solar emission spectrum of only 16%,[35] Nd:YAG has been demonstrated as the best laser material under highly intense solar pumping because of its excellent characteristic on thermal conductivity ($K = 14$ W/m.K[37]), high quantum efficiency, and fracture strength ($\sigma_{max} = 200$ N/mm^2[32]) compared with other host materials. For 1.0% Nd:YAG laser medium, 22 peak absorption wavelengths[15–18] were defined in ZEMAX® numerical data. The peak wavelengths and their respective absorption coefficients, listed in Table 1, were added to the glass catalog for Nd:YAG material. Solar irradiance values for the 22 absorption peaks could be consulted from the standard solar spectra for AM1.5 and saved as source wavelength data.

Table 1 Peak absorption wavelengths and their respective absorption coefficients of the 1.0 at. % Nd:YAG material.[15–18]

Wavelength (nm)	527	531	568	578	586	592	732	736	743	746	753
Absorption coefficients (cm^{-1})	1.43	1.35	2.41	0.94	5.88	1.43	1.43	2.41	1.83	6.21	3.73
Wavelength (nm)	758	790	793	803	805	808	811	815	820	865	880
Absorption coefficients (cm^{-1})	3.24	1.05	2.88	3.22	2.81	6.91	4.27	1.39	1.90	1.43	0.92

In ZEMAX® nonsequential ray-tracing, the laser rod was divided into a total of 18,000 voxels. The path length in each voxel was then found. With this value and the effective absorption coefficient of the 1.0 at. % Nd:YAG material, the absorbed solar pump power within the laser medium was numerically calculated by summing up the absorbed pump radiation of all zones.

3.2 *Optimization of the Laser Resonator Parameters Through LASCAD™*

The absorbed pump flux data from the ZEMAX® analysis was then processed by LASCAD™ (LASer Cavity Analysis and Design) software to study the laser resonator beam parameters and quantify the thermal effects applied in the active medium. It was also based on the LASCAD™ results that the design parameters in ZEMAX® were optimized more accurately.

The stimulated emission cross section of 2.8×10^{-19} cm^2,[32] the fluorescence lifetime of 230 μs,[32] and a typical absorption and scattering loss of 0.003 cm^{-1} for the 1.0 at. % Nd:YAG medium were adopted in LASCAD™ analysis. The mean absorbed and intensity-weighted solar pump wavelength of 660 nm was also used in the analysis.[12] In LASCAD™ program, the optical resonator was comprised of two opposing parallel mirrors at right angles to the axis of the active medium, as illustrated in Fig. 7.

One end mirror represents the high reflection coating (HR 1064 nm, 99.98%) on the upper end face of the rod (Fig. 4), for the laser emission wavelength of Nd:YAG. The output coupler, on the right side, is partial reflection coated (PR 1064 nm, usually 90% to 98%). The amount of feedback was determined by the reflectivity of the PR mirror. Here, L represents the separation length of the PR mirror to the lower end face of the laser rod (Fig. 4), which is antireflection (AR 1064 nm) coated. As shown in Fig. 7, resonator length is a key parameter for the efficient

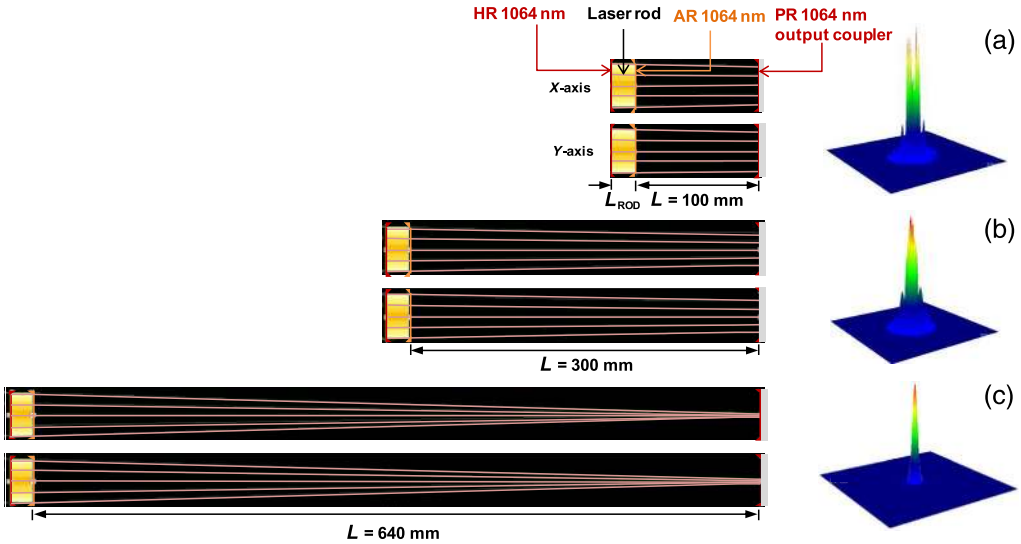

Fig. 7 Laser resonator design in LASCAD™ analysis at different length (L) and correspondingly numerical output laser beam profiles from a 3.5-mm-diameter Nd:YAG rod. Laser beam profile at (a) L = 100 mm, (b) L = 300 mm, and (c) L = 640 mm.

extraction of TEM_{00}-mode laser power due to the power-dependent thermal lensing of the laser material. Pump power–induced fluctuations on the rod's thermal focal length exert strong influence on resonator modes configuration and stability, giving rise to thermally stable zones.[32,37] Conventionally, lasers are designed to operate at the middle of thermally stable zones, where the fundamental mode size is insensitive to thermal perturbation.[32,38] Since, the TEM_{00}-mode Gaussian beam has the smallest beam size and divergence in a resonator, if its size is much smaller than the transverse size of the gain region, which happens for laser resonators with relatively small L, the TEM_{00}-Gaussian beam mode will poorly match the gain region, and laser will oscillate at several modes,[32] as shown in Fig. 7(a). This comes at the expense of high M^2 factors. As L increases, the TEM_{00}-mode size within the rod increases and higher order modes are suppressed by large diffraction losses at the rod edges. Consequently, fewer order modes oscillate, as shown in Fig. 7(b). As laser operates closer to the border of the resonator stable zone, for long L in Fig. 7(c), the TEM_{00}-mode size becomes more sensitive to thermal focus fluctuations and increases toward an asymptote.[37] Thus, spatial overlap between TEM_{00}-mode and pump mode volumes become larger, and the few-order modes are also suppressed, giving rise to only one mode. The parameter L, together with the PR mirror reflectivity (R) and the radius of curvature (RoC), was optimized to achieve the highest TEM_{00}-mode laser power and, thus, the lowest laser beam divergence.

4 Advances in Multimode Solar Laser Performance

In LASCAD™ analysis, for multimode laser oscillation, an optical resonator with $L = 100$ mm and RoC $= -10$ m output mirror was defined, as shown in Fig. 7(a). The multimode laser power as a function of the laser rod diameter from the four-rod scheme is shown in Fig. 8. These numerical results are compared to the numerical results of the previous single-laser head[18] with the same solar collector area of 3.07 m^2. The solar irradiance of 1000 W/m^2 was considered in both cases.

With the previous single-laser head, the maximum multimode laser power of 55.70 W was numerically achieved for $D_{ROD} = 6.0$ mm, resulting in the collection efficiency of 18.14 W/m^2. With the four-rod scheme, the total multimode power of 59.04 W was achieved by pumping four small diameter ($D_{ROD} = 3.5$ mm) Nd:YAG rods simultaneously, leading to 19.23 W/m^2 collection efficiency. Although this value was only slightly higher than the numerical result of the previous single-laser head, it is worth noting that the four-rod scheme allowed an efficient pumping of small diameter rods. This enabled an easy production of TEM_{00}-mode laser, as discussed in Sec. 5.

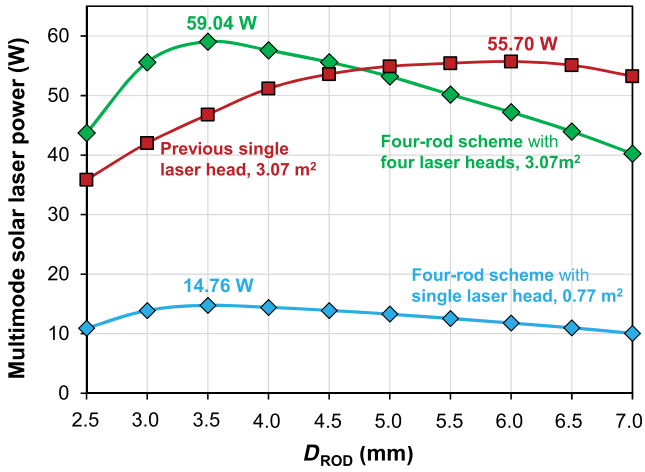

Fig. 8 Multimode laser power as a function of the laser rod diameter (D_{ROD}), numerically obtained by both the four-rod scheme and the previous single-laser head[18] with 3.07 m^2 collection area.

5 Advances in TEM_{00}-Mode Solar Laser Performance

5.1 *Improvement in TEM_{00}-Mode Power, Collection Efficiency, and Brightness Conversion Efficiency*

The dependency of TEM_{00}-mode power on the semivertex angle of the pyramidal reflector was first studied. As shown in Fig. 9, the maximum TEM_{00}-mode power of 7.22 W was achieved by $\alpha = 10$ deg. By reducing α, the laser head approached more closely to the pyramidal reflector (Fig. 4). Consequently, for $\alpha < 10$ deg, the biconical lens became less efficient in compressing the solar rays to the laser rod, resulting also in a more considerable decrease in TEM_{00}-mode power, as compared to that achieved by $\alpha > 10$ deg.

The TEM_{00}-mode laser power from a single-laser head by four-rod pumping approach was numerically studied as a function of both the laser rod diameter and length, as represented in Fig. 10. The parameters of the biconical lens and conical pump cavity were optimized in order to find the best symmetry of the M_x^2, M_y^2 beam quality factors for each laser rod. The Nd:YAG rods with $D_{ROD} = 3.0$ to 3.5 mm and $L_{ROD} = 20$ to 30 mm offered the best TEM_{00}-mode powers. In these cases, the TEM_{00}-mode power varied slightly, as shown in Fig. 10. The maximum TEM_{00}-mode power of 7.22 W was achieved by pumping a $D_{ROD} = 3.0$ mm, $L_{ROD} = 20$ mm Nd:YAG rod. Since a single-laser rod was pumped by only one-fourth of the total collection area (0.77 m^2) of the parabolic mirror, the maximum collection efficiency of 9.41 W/m^2 was achieved by each laser rod, being 1.19 times more than the previous

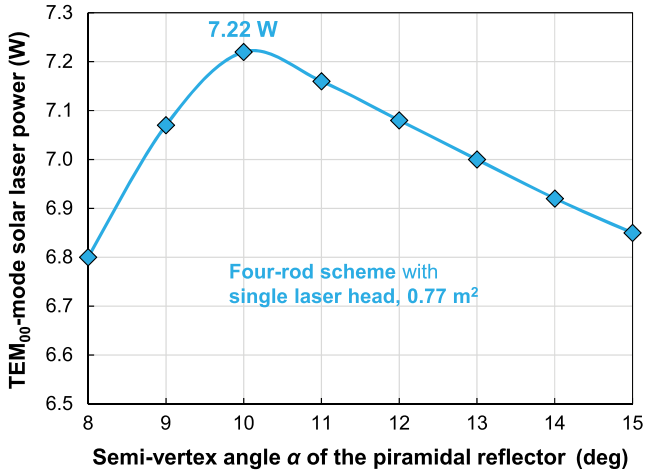

Fig. 9 TEM_{00}-mode laser power as a function of the pyramidal semivertex angle α.

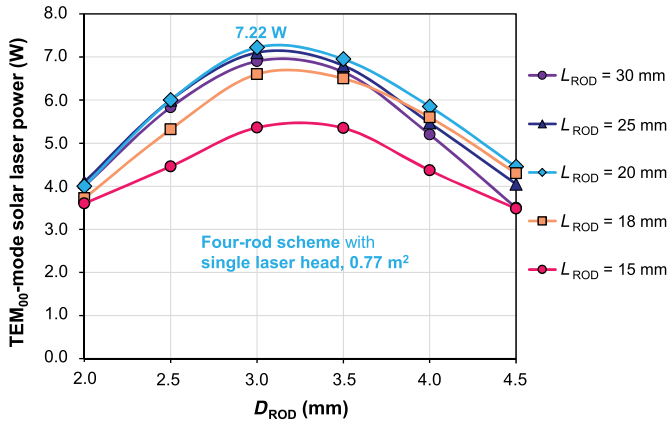

Fig. 10 TEM_{00}-mode laser power as a function of the laser rod diameter (D_{ROD}) and length (L_{ROD}), numerically obtained from a single-laser head of the four-rod scheme.

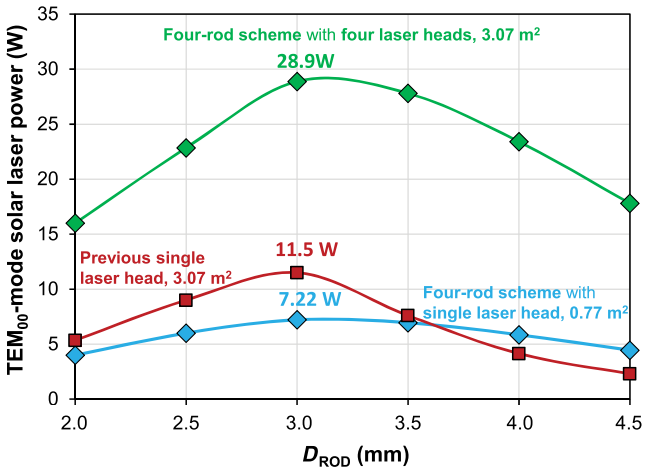

Fig. 11 TEM_{00}-mode laser power as a function of D_{ROD}, numerically obtained from both the four-rod scheme and the previous single-laser head[18] with 3.07 m^2 collection area.

experimental record.[18] Also, the brightness conversion efficiency of 0.86% was numerically calculated, representing 1.56 times enhancement over the previous experimental record.[18]

The numerically calculated TEM_{00}-mode laser performance of the four-rod pumping approach was also compared to the numerical result of the previous single-laser head[18] by the same solar collector with 3.07 m^2 collection area, as shown in Fig. 11. From a single-laser head of the four-rod scheme, the maximum TEM_{00}-mode power of 7.22 W was numerically obtained from the $D_{ROD} = 3.0$ mm rod. Therefore, the total TEM_{00}-mode power of about 29 W (4×7.22 W) was obtained from the four-rod scheme, being 2.5 times higher than the numerical result of the previous single-laser head, with 11.5 W TEM_{00}-mode laser power. About 2.5 times enhancement in TEM_{00}-mode collection efficiency was also obtained by the four-rod scheme. Due to the substantial improvement in TEM_{00}-mode power, the brightness conversion efficiency was 2.3 times more than the numerical result of the previous single-laser head. It is also worth noting that for $D_{ROD} > 3.5$ mm, a single-laser head of the four-rod scheme produced higher TEM_{00}-mode power than the numerical results of the previous single-laser head.

5.2 *Improvement in TEM_{00}-Mode Laser Beam Stability*

The numerically calculated multimode and TEM_{00}-mode powers, as well as their respective laser beam profiles, as a function of the solar irradiance for both schemes are shown in Fig. 12. The multimode and TEM_{00}-mode powers numerically obtained at the solar irradiances of 700, 800, 900, and 1000 W/m^2 are also represented in Table 2 for both schemes. The corresponding TEM_{00}-mode power/multimode power ratio is also indicated.

As shown in Fig. 12 and Table 2, the numerical TEM_{00}-mode laser power from the previous single-laser head was found to be much more sensitive to the variation of solar irradiance. The same is verified for the TEM_{00}-mode power/multimode power ratio. At solar irradiance of 700 W/m^2, 2.55 W TEM_{00}-mode power was numerically achieved from the previous single-laser head, representing only 34.4% power ratio. Therefore, the oscillation of several modes was numerically obtained, as shown by the multimode laser beam profile in Fig. 12. As solar irradiance increased, only few modes began to oscillate. Low-order mode laser beam profile was reduced to only one mode when the solar irradiance approached 1000 W/m^2. In this case, 11.5 W TEM_{00}-mode and 11.7 W multimode powers were numerically attained, representing a high power ratio of 98.3%. At the solar irradiance of 1000 W/m^2, the laser was operating close to the edge of the optically stable region. Therefore, a slight increase in solar irradiance led to a shorter thermal length and, consequently, to the extinction of laser output power.

For the four-rod scheme, the TEM_{00}-mode power had increased by 2.6 times with the variation of solar irradiance from 700 to 1000 W/m^2. Yet, the laser beam profiles remained a near-Gaussian shape. Therefore, TEM_{00}-mode power was dominant in laser emission, even at low

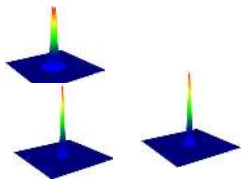

Table 2 TEM_{00}-mode laser and multimode laser powers numerically obtained from both schemes, at different solar irradiances. The respective TEM_{00}-mode power/multimode power ratios are also indicated.

Solar irradiance	700 W/m^2	800 W/m^2	900 W/m^2	1000 W/m^2
Four-rod scheme				
TEM_{00}-mode power (W)	11.0	14.5	20.5	28.9
Multimode power (W)	13.0	16.4	21.8	29.1
TEM_{00}-mode power/multimode power ratios (%)	84.6	88.5	93.7	99.2
Previous single-laser head				
TEM_{00}-mode power (W)	2.55	3.49	5.30	11.5
Multimode power (W)	7.40	7.87	8.70	11.7
TEM_{00}-mode power/multimode power ratios (%)	34.4	44.4	60.9	98.3

solar irradiance of 700 W/m^2. About 84.6% power ratio was obtained in this case, indicating a substantial improvement in TEM_{00}-mode laser beam stability as compared to the previous single-laser head.

5.3 *Improved TEM_{00}-Mode Thermal Performance*

The main problem hindering the solar lasers performance is the heat generation within the active medium, which leads to a spatial variation in temperature and internal stress within the laser

ERROR: undefined
OFFENDING COMMAND: ~

STACK:

-savelevel-